Dibenzo-p-dioxin

Twisted and puckered excited state molecular geometries

Spanget-Larsen, Jens

Published in:
Computational and Theoretical Chemistry

DOI:
10.1016/j.comptc.2019.112551

Publication date:
2019

Document Version
Peer reviewed version

Citation for published version (APA):
Spanget-Larsen, J. (2019). Dibenzo-*p*-dioxin: Twisted and puckered excited state molecular geometries. *Computational and Theoretical Chemistry*, *2019*(1164), [112551]. https://doi.org/10.1016/j.comptc.2019.112551

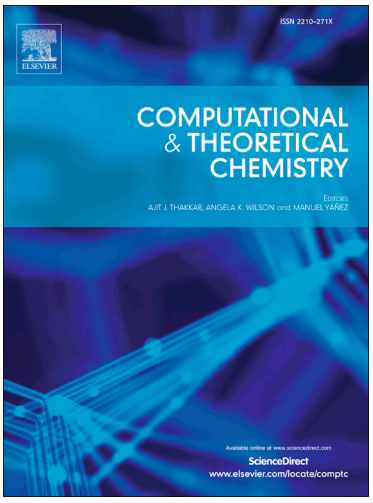

Dibenzo-*p*-dioxin. Twisted and puckered excited state molecular geometries

Jens Spanget-Larsen

PII: S2210-271X(19)30245-2
DOI: https://doi.org/10.1016/j.comptc.2019.112551
Reference: COMPTC 112551

To appear in: *Computational & Theoretical Chemistry*

Received Date: 28 June 2019
Revised Date: 23 July 2019
Accepted Date: 25 July 2019

Please cite this article as: J. Spanget-Larsen, Dibenzo-*p*-dioxin. Twisted and puckered excited state molecular geometries, *Computational & Theoretical Chemistry* (2019), doi: https://doi.org/10.1016/j.comptc.2019.112551

Dibenzo-*p*-dioxin. Twisted and puckered excited state molecular geometries

Jens Spanget-Larsen

Department of Science and Environment, Roskilde University, Universitetsvej 1, DK-4000 Roskilde, Denmark.

Keywords

Dibenzo-*p*-dioxin
Excited state nuclear configurations
Density functional theory (DFT)
Time-dependent DFT
Double hybrid methods
Configuration interaction
Triplet spin populations

ABSTRACT. The title compound is generally acknowledged to have a planar D_{2h} symmetrical molecular geometry in the ground state S_0, and previous theoretical and experimental investigations seem to support the assumption of similar planar geometries in the excited singlet and triplet electronic states, S_1 and T_1. But a variety of theoretical models predict non-planar equilibrium geometries for these states: In the lowest excited singlet state (S_1) a twisted, propeller-like geometry with D_2 symmetry is predicted, while a strongly puckered, biradicaloid dienediyl-like structure is predicted for the triplet state (T_1).

E-mail address: Spanget@ruc.dk (J. Spanget-Larsen)

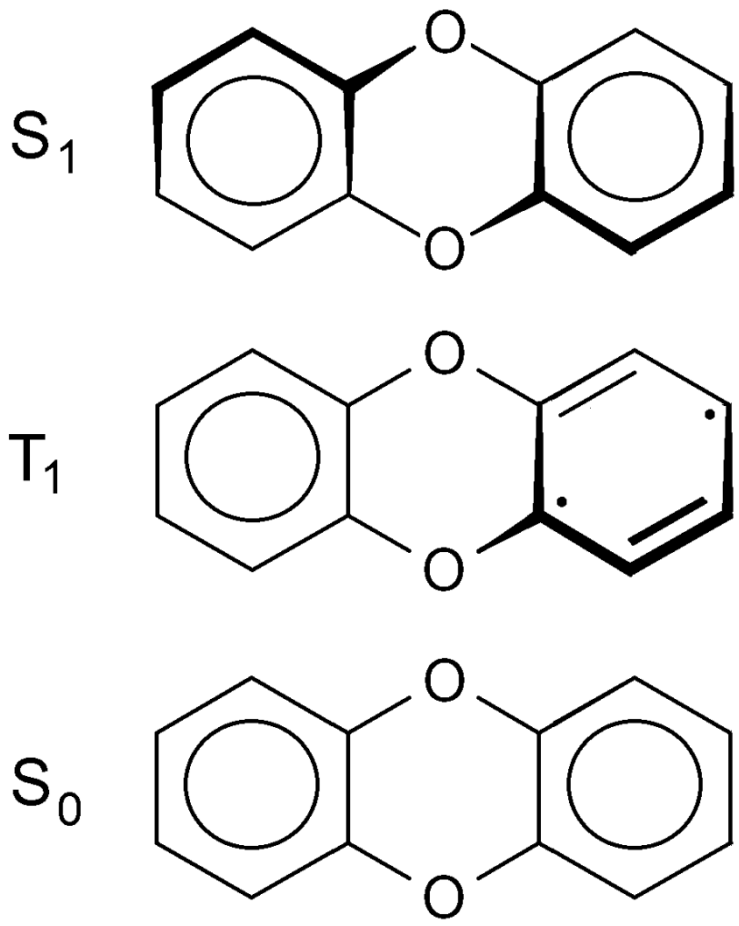

Graphical abstract

Highlights

- Excited state molecular geometries calculated with a variety of theoretical models
- Predictions at variance with previous assumptions of planar geometries
- Twisted D_2 symmetrical structure predicted for the S_1 state of dibenzo-*p*-dioxin
- Puckered dienediyl-like structure predicted for the T_1 state of dibenzo-*p*-dioxin

1. Introduction

The molecular structure of dibenzo-*p*-dioxin (DD, Scheme 1) was a matter of controversy for many years. In particular, it was discussed whether the molecule in the S_0 ground state had a planar D_{2h} symmetrical structure or a non-planar "butterfly" conformation with C_{2v} symmetry (see Refs. [1-5] and literature cited therein). The question was apparently settled in 2002 when Gastilovich et al. [1] analyzed a collection of spectroscopic data and concluded that the ground state had a planar D_{2h} symmetrical nuclear configuration. Similar planar molecular geometries were deduced by Gastilovich et al. [1] for the excited electronic singlet and triplet states, S_1 and T_1. These results were subsequently supported by Ljubić and Sabljić [3] who performed *ab initio* multi-configurational CASSCF/CASPT2 calculations of several valence excited states of DD. On the basis of harmonic analyses the authors concluded that "all of the π-π* excited states exhibit planar D_{2h} minima" [3].

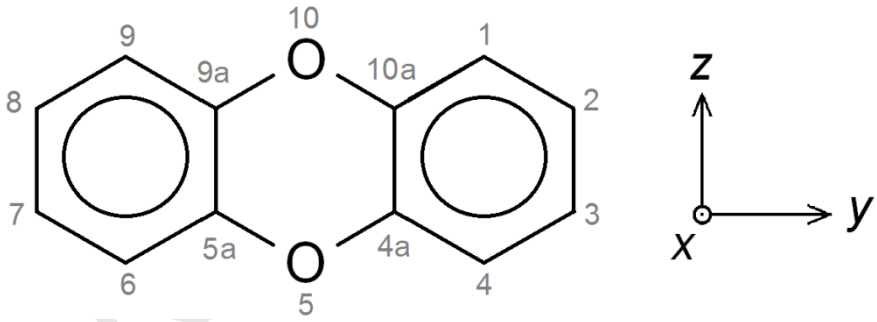

Scheme 1. Dibenzo-*p*-dioxin (DD) with atom numbering and definition of molecular coordinate system for the D_{2h} symmetrical ground state geometry.

We recently published the results of a polarization spectroscopic investigation of the electronic transitions of DD [6], leading to revision of previous assignments. It was found that time dependent density functional theory (TD-DFT) [7-9] calculations using the CAM-B3LYP [10] functional provided an adequate description of the observed vertical transitions and their polarization directions. Under the assumption of D_{2h} molecular symmetry, the lowest vertically excited singlet state S_1 was predicted to be 1^1B_{3g} [6], in consistency with the results of Ljubić and Sabljić [3]. But a subsequent TD–CAM-B3LYP calculation of the

molecular equilibrium geometry for this state indicated distortion to a non-planar structure with lower symmetry. A similar result was obtained for the T_1 state with CAM-B3LYP. These predictions were unexpected in view of the previously reported conclusions by Gastilovich et al. [1] and by Ljubić and Sabljić [3]. It was thus decided to repeat the calculations with a selection of different theoretical procedures in order to check the TD–CAM-B3LYP and CAM-B3LYP predictions. The present publication reports the results of this project. Additional information is provided as Supplementary data, referred to in the ensuing text as S1-S7.

3. Calculations

All quantum chemical calculations were performed by using the GAUSSIAN16 software package [11]. The S_1 state was computed with the CIS configuration interaction (CI) procedure [12], the TD–Hartree-Fock (TD-HF) procedure [13], and the TD-DFT [7-9] procedure with the functionals B3LYP [14], CAM-B3LYP [10], and ωB97XD [16]. The T_1 state was computed with the Hartree-Fock methods UHF and ROHF [17-19], the CI procedures CID and CISD [20-22], the DFT procedures B3LYP [14,15], CAM-B3LYP [10], M06 [23], and ωB97XD [16], and the double hybrid procedures B2PLYP [24] and B2PLYP-D3 [25,26]. The CAM-B3LYP calculation was performed also with inclusion of a solvent contribution by using the polarizable continuum model (PCM, ethanol) [9,27]. The basis set was 6-311++G(d,p), except for CID and CISD where the basis was reduced to 6-311G(d,p) [9,11]. Geometry optimizations were performed with and without the restriction of planar D_{2h} symmetry. Attempts to optimize the T_1 geometry with Møller-Plesset 2-order perturbation theory (MP2) [28,29] were unsuccessful. However, an MP2-like contribution is included in the double hybrid B2PLYP methods [24-26]. The optimized S_1 and T_1 geometries were characterized by harmonic analyses, except for CID, CISD, and B2PLYP-D3 where the analyses were not feasible. The computed wavefunctions were analyzed by the natural bond orbital (NBO) procedure [30], providing NBO Wiberg bond indices [31] and NBO triplet

spin populations. Selected parameters are listed in Tables 1 and 2. A number of more detailed results are given as Supplementary data, S1-S7: TD–CAM-B3LYP data for the S_1 state, symmetries D_{2h} and D_2 (S1-S2); CAM-B3LYP data for the T_1 state, symmetries D_{2h} and C_1 (S3-S4); APFD, B2PLYP, and CISD data for the T_1 state, symmetry C_1 (S5-S7).

4. Results and Discussion

4.1 Singlet state S_1

Under the assumption of planar D_{2h} symmetrical molecular geometry, the lowest excited singlet state S_1 of DD predicted by TD–CAM-B3LYP is well-described by promotion of an electron from the $3b_{3u}(\pi)$ to the $2a_u(\pi*)$ molecular orbital (Fig. 1), giving rise to an 1^1B_{3g} state [6] (S1). This is consistent with the result of the CASSCF/CASPT2 calculation published by Ljubić and Sabljić [3]. But a harmonic analysis of the relaxed, planar TD–CAM-B3LYP geometry reveals one imaginary frequency, corresponding to an out-of-plane twisting vibration of a_u symmetry involving the carbon nuclei of the dioxin moiety (S1). A feature at 155 cm^{-1} in the phosphorescence spectrum of DD was assigned by Gastilovich et al. [1] to the corresponding a_u ground state fundamental. The prediction of an imaginary frequency for this mode indicates that the planar configuration is a transition structure. Optimization of the excited state geometry leads to a non-planar, twisted equilibrium configuration with D_2 symmetry (S2). The 1^1B_{3g} state is transformed to an 1^1B_2 state in the D_2 equilibrium geometry (using the coordinate systems indicated in Schemes 1 and 2), thereby lowering the electronic energy of the system by 0.83 kcal/mol. Hence, the planar D_{2h} transition structure is interrelating two equivalent D_2 symmetrical equilibrium structures with a transition energy corresponding to rapid equilibration at room temperature.

The computed molecular equilibrium geometry is shown in Fig. 2. The two carbocyclic rings are nearly planar, and bond lengths and Wiberg bond indices are insignificantly affected by the transformation from D_{2h} to D_2 geometry (S1, S2). The

distortion is essentially limited to the central dioxin ring where the O-C-C-O dihedral angles are twisted by 21°. The twisting can be explained in part by inspection of the MO amplitudes in Fig 1: $3b_{3u}(\pi)$ and $2a_u(\pi*)$ are bonding and antibonding, respectively, with respect to the C-C linkages of the dioxin moiety. Promotion of an electron from $3b_{3u}(\pi)$ to $2a_u(\pi*)$ thus dilutes the π bonding character of these linkages, thereby reducing the tendency to planarity of the dioxin moiety in the excited state. A similar inversion distortion was predicted by Lee et al. [4] for the radical anion of DD.

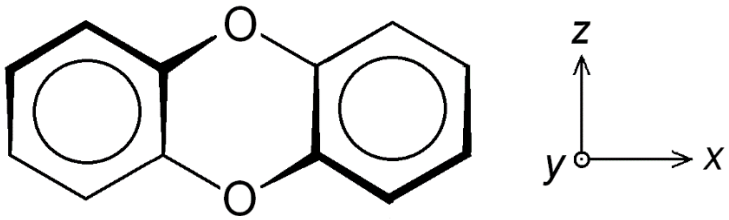

Scheme 2. Definition of molecular coordinate system for the propeller-shaped, D_2 symmetric molecular geometry predicted for the excited singlet state S_1 of dibenzo-*p*-dioxin (DD).

The TD–CAM-B3LYP result is at variance with previous conclusions [1-3]. The calculation was therefore repeated with a number of different theoretical procedures, see Section 3 for details. All of them predict D_2 symmetrical S_1 equilibrium geometries, thereby supporting the TD–CAM-B3LYP results discussed above. As listed in Table 1, the predicted O-C-C-O distortion angles range from 14° to 21°, and the energy differences $\Delta E = E(1^1B_{3g}) - E(1^1B_2)$ between the relaxed, planar configuration (D_{2h}) and the non-planar equilibrium geometry (D_2) range from 0.31 to 1.00 kcal mol^{-1}.

4.2 Triplet state T_1

Under the assumption of planar D_{2h} symmetrical molecular geometry, the lowest triplet state T_1 of DD predicted with CAM-B3LYP is the 1^3B_{3g} state (S3), consistent with the results of Ljubić and Sabljić [3]. But as in the case of the related singlet state 1^1B_{3g}, the harmonic analysis reveals one imaginary frequency corresponding to an out-of-plane vibration of a_u symmetry (S3). Full optimization of the geometry leads to a strongly distorted,

non-planar equilibrium geometry with complete loss of symmetry, and with a biradicaloid dienediyl-like spin distribution localized in one of the carbocyclic rings, as indicated in Scheme 3 (S4). The resulting 1^3A triplet state is lowered by 7.94 kcal mol^{-1} relative to the 1^3B_{3g} state of the relaxed, planar D_{2h} configuration. The redistribution of the electron density creates a dipole moment of 0.89 Debye (S4). Approximating the influence of an alcoholic solvent by means of the PCM model (solvent=ethanol) does not substantially affect the results of the calculation: The calculated molecular geometry is essentially unchanged, the energy lowering is increased from 7.94 to 8.17 kcal mol^{-1}, and the dipole moment is increased from 0.89 to 1.21 Debye.

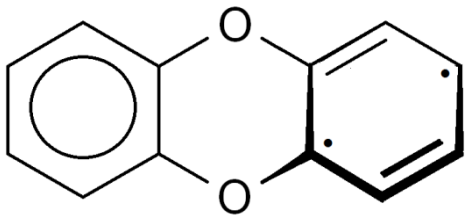

Scheme 3. Approximate representation of the puckered, biradicaloid molecular geometry predicted for the triplet state T_1 of dibenzo-*p*-dioxin (DD).

The CAM-B3LYP equilibrium geometry for the 1^3A state is shown in Fig. 3. It is apparent that the two carbocyclic rings are essentially planar, while the dioxin moiety is strongly puckered. In particular, one of the O-C-C-O the dihedral angles is predicted to be as large as 42° (here taken as O5-C4a-C10a-O10). The bond lengths and Wiberg bond indices indicate that one of the benzene rings is basically intact, while the other is transformed to a dienediyl-like structure (S4). The NBO analysis reveals large spin populations on the C4a and C2 centers, *s*(C4a) = 0.74 and *s*(C2) = 0.58 (Fig. 4). The C4a carbon appears as a fairly well-developed, pyramidalized radical center, linked with essential single bonds to the neigbouring atoms. Atomic coordinates, NBO net charges and spin populations, dipole moment, bond lengths, and NBO Wiberg bond indices are given in S4.

The results of the CAM-B3LYP calculation are in strong disagreement with previous conclusions concerning the molecular and electronic structure of the T_1 state of DD [1,3]. But

the main results of the calculation are supported by those of about a dozen different theoretical procedures, including HF, DFT, and CI methods (Section 3). All the applied procedures predict distortion to a puckered, low-symmetry structure with a dienediyl-like spin distribution, consistent with the results discussed above for CAM-B3LYP. As listed in Table 2, O5-C4a-C10a-O10 distortion angles are predicted in the range 38-51°, NBO spin populations *s*(C4a) and *s*(C2) in the ranges 0.66-0.88 and 0.51-0.80, respectively, and dipole moments in the range 0.36-0.89 Debye (1.21 Debye for CAM-B3LYP + PCM). However, the computed energy differences $\Delta E = E(1^3B_{3g}) - E(1^3A)$ vary widely. Detailed T_1 results for CAM-B3LYP, APFD, B2LYP, and CISD are provided in S3 – S7.

5. Conclusions

The photophysical properties of dibenzo-*p*-dioxin (DD) and its derivatives have been investigated for many years under the explicit assumption that the S_0 ground state and the excited electronic states S_1 and T_1 have planar D_{2h} symmetrical molecular geometries [32-38]. However, the theoretical results presented in this publication provide strong evidence for non-planar equilibrium geometries in the S_1 and T_1 states. Most remarkably, a strongly distorted nuclear configuration with a puckered dioxin moiety and a dienediyl-like spin distribution is predicted for the T_1 state. The results are confirmed by the application of a variety of theoretical procedures, including Hartree-Fock, density functional, double hybrid, and configuration interaction procedures. The predictions are controversial, particularly for the T_1 state, and should be checked by further studies. For example, the use of larger, correlation consistent basis sets should be considered, particularly in the case of the post-HF calculations. But it cannot be excluded that the interpretation of the photophysical properties of DD and its derivatives needs revision in view of the results presented in this publication.

Competing interests

The author declares no competing interests.

Appendix A. Supplementary data

Supplementary data to this article can be found online at . . .

Table 1. Calculated singlet state S_1 dihedral angles Φ(O-C-C-O) and electronic energy differences $\Delta E = E(1^1B_{3g}) - E(1^1B_2)$ between the relaxed, planar configuration (D_{2h}) and the non-planar equilibrium geometry (D_2).

Method	Φ	ΔE / kcal mol^{-1}
TD–HF	14°	0.39
TD–B3LYP	16°	0.31
CIS	17°	1.00
TD–CAM-B3LYP	21°	0.83
TD–ωB97XD	21°	0.69

Table 2. Calculated triplet state T_1 dihedral angles Φ(O5-C4a-C10a-O10), NBO spin populations *s*(C4a) and *s*(C2), dipole moments M, and energy differences $\Delta E = E(1^3B_{3g}) - E(1^3A)$ between the relaxed, planar configuration (D_{2h}) and the non-planar equilibrium geometry (C_1).

Method	Φ	*s*(C4a)	*s*(C2)	M / Debye	ΔE / kcal mol^{-1}
B3LYP	38°	0.66	0.51	1.15	1.60
M06	38°	0.67	0.54	0.93	1.87
APFD	38°	0.69	0.53	1.01	2.19
ROHF	39°	0.82	0.75	0.36	35.17
B2PLYP	42°	0.78	0.64	0.49	0.02
CAM-B3LYP	42°	0.74	0.58	0.89	7.94
CAM-B3LYP + PCM [a]	43°	0.74	0.58	1.21	8.17
B2PLYP-D3	43°	0.78	0.64	0.49	0.08
ωB97XD	43°	0.74	0.57	0.88	8.00
CISD	44°	0.88	0.80	0.39	22.03
CID	51°	0.88	0.80	0.39	21.85
UHF	51°	0.86	0.79	0.61	39.07

[a] Solvent effect included by using the PCM model, solvent=ethanol, see text.

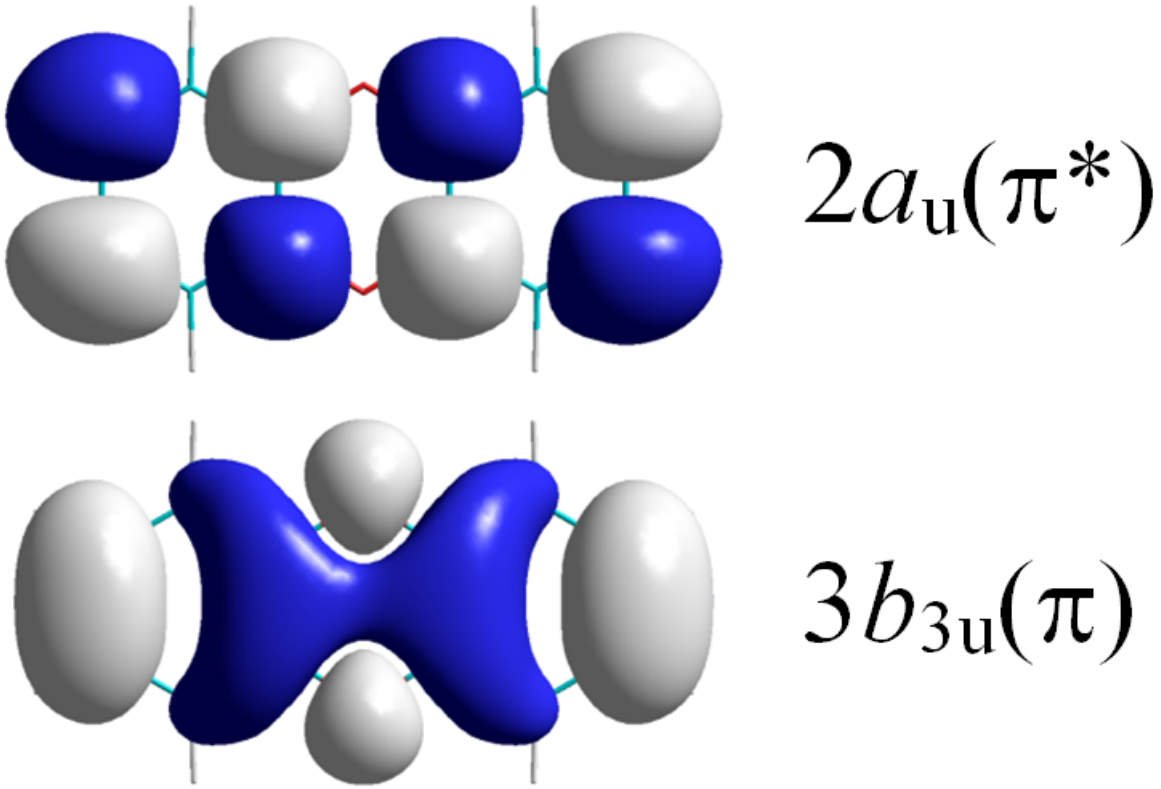

Fig. 1. Diagrams of the highest occupied and lowest unoccupied π type MOs for planar D_{2h} symmetrical dibenzo-*p*-dioxin (DD) predicted with CAM-B3LYP [6].

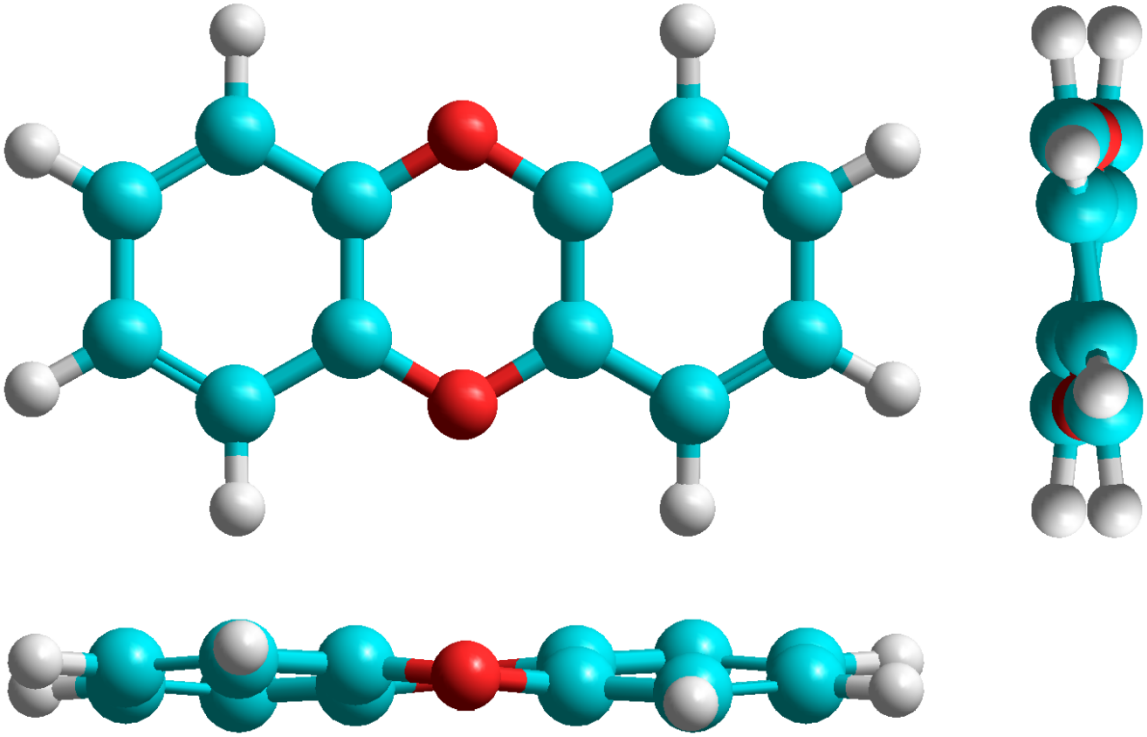

Fig. 2. Molecular equilibrium geometry of dibenzo-*p*-dioxin (DD) in the S_1 singlet state (1^1B_2) predicted with TD–CAM-B3LYP. The structure is viewed along the three different axes of symmetry in the D_2 point group.

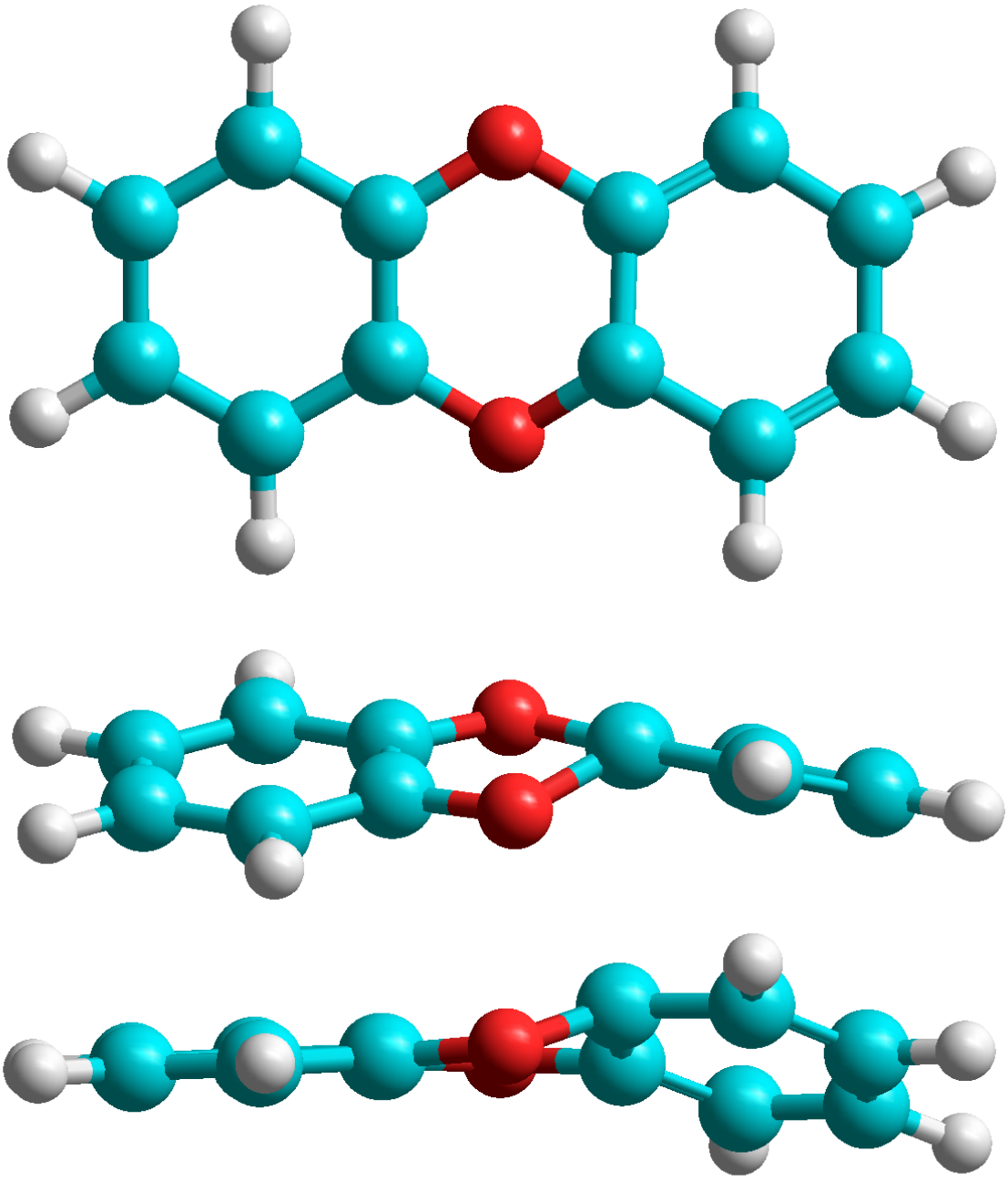

Fig. 3. Molecular equilibrium geometry of dibenzo-*p*-dioxin (DD) in the T_1 triplet state (1^3A) predicted with CAM-B3LYP. In the two lowest diagrams, the structure is viewed along the C4a–C10a and C5a–C9a bond axes, respectively.

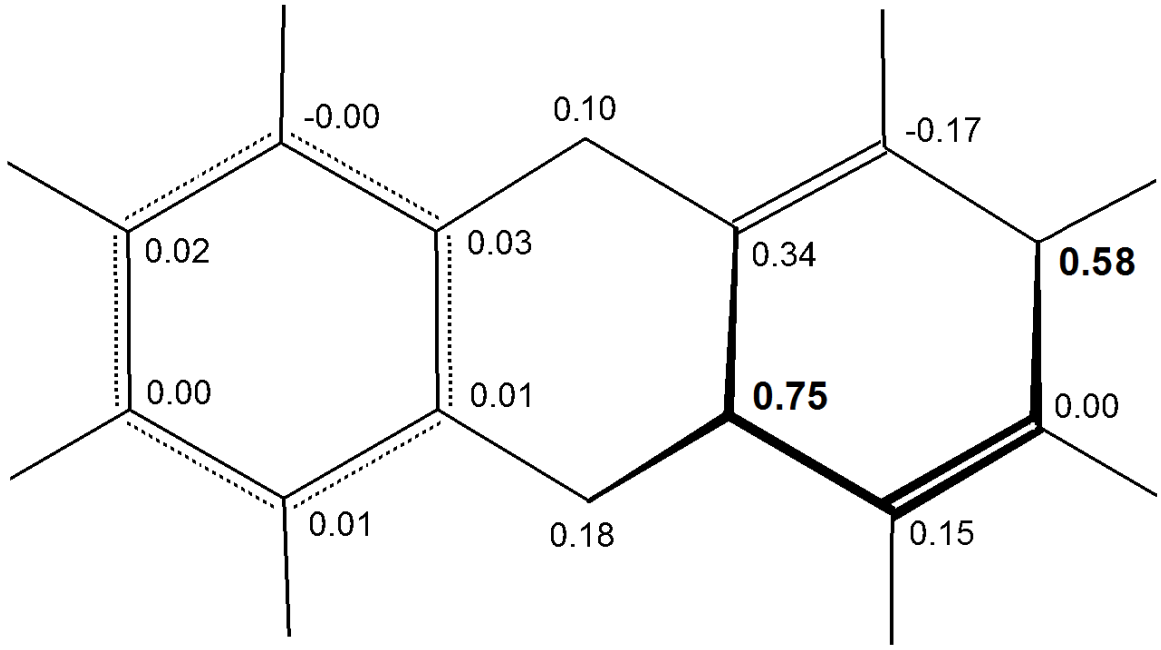

Fig 4. NBO spin populations for the T_1 triplet state (1^3A) of dibenzo-*p*-dioxin computed with CAM-B3LYP.

References

1 E.A. Gastilovich, V. G. Klimenko, N.V. Korol'kova, R.N. Nurmukhametov, Spectroscopic data on nuclear configuration of dibenzo-*p*-dioxin in S_0, S_1, and T_1 electronic states, Chem. Phys. 282 (2002) 265-275.

2 M. Baba, A. Doi, Y. Tatamitani, S. Kasahara, H. Kato, Sub-doppler high-resolution excitation spectroscopy of dibenzo-*p*-dioxin, J. Phys. Chem. A 108 (2004) 1388-1392.

3 I. Ljubić, A. Sabljić, Dibenzo-*p*-dioxin. An ab initio CASSCF/CASPT2 study of the π–π* and *n*–π* valence excited states, J. Phys. Chem. A 109 (2005) 8209-8217.

4 J.E. Lee, W. Choi, S. Odde, B.J. Mhin, K. Balasubramanian, Electron affinity and inversion distortion of dibenzo-*p*-dioxin, Chem. Phys. Lett. 410 (2005) 142-146.

5 T.K. Eriksen, B.K.V. Hansen, J. Spanget-Larsen, The vibrational structure of dibenzo-*p*-dioxin. IR linear dichroism, Raman spectroscopy, and quantum chemical calculations, Polish J. Chem. 82 (2008) 921-934.

6 D.D Nguyen, N.C. Jones, S.V. Hoffmann, J. Spanget-Larsen, Electronic states of dibenzo-*p*-dioxin. A synchrotron radiation linear dichroism investigation, Chem. Phys. 519 (2019) 64-68.

7 M.E. Casida, Review: Time-dependent density-functional theory for molecules and molecular solids, J. Mol. Struct. THEOCHEM 914 (2009) 3-18.

8 C. Adamo, D. Jacquemin, The calculations of excited-state properties with Time-Dependent Density Functional Theory, Chem. Soc. Rev. 42 (2013), 845-856.

9 J.B. Foresman, Æ. Frisch, Exploring chemistry with electronic structure methods, Third Edition, Gaussian, Inc., Wallingford CT, 2015.

10 T. Yanai, D. Tew, N.A. Handy, New hybrid exchange-correlation functional using the Coulomb-attenuating method (CAM-B3LYP), Chem. Phys. Lett. 393 (2004) 51-57.

11 M.J. Frisch, G.W. Trucks, H.B. Schlegel, G.E. Scuseria, M.A. Robb, J.R. Cheeseman, G. Scalmani, V. Barone, G.A. Petersson, H. Nakatsuji, X. Li, M. Caricato, A.V. Marenich, J. Bloino, B.G. Janesko, R. Gomperts, B. Mennucci, H.P. Hratchian, J.V. Ortiz, A.F. Izmaylov, J.L. Sonnenberg, D. Williams-Young, F. Ding, F. Lipparini, F.

Egidi, J. Goings, B. Peng, A. Petrone, T. Henderson, D. Ranasinghe, V.G. Zakrzewski, J. Gao, N. Rega, G. Zheng, W. Liang, M. Hada, M. Ehara, K. Toyota, R. Fukuda, J. Hasegawa, M. Ishida, T. Nakajima, Y. Honda, O. Kitao, H. Nakai, T. Vreven, K. Throssell, J.A. Montgomery, Jr., J.E. Peralta, F. Ogliaro, M.J. Bearpark, J. J. Heyd, E.N. Brothers, K.N. Kudin, V.N. Staroverov, T.A. Keith, R. Kobayashi, J. Normand, K. Raghavachari, A.P. Rendell, J.C. Burant, S.S. Iyengar, J. Tomasi, M. Cossi, J.M. Millam, M. Klene, C. Adamo, R. Cammi, J. W. Ochterski, R.L. Martin, K. Morokuma, O. Farkas, J.B. Foresman, D.J. Fox, Gaussian16, Revision A.03, Gaussian, Inc., Wallingford CT, 2016.

12 J.B. Foresman, M. Head-Gordon, J.A. Pople, M.J. Frisch, Toward a systematic molecular orbital theory for excited states, J. Phys. Chem. 96 (1992) 135-49.

13 P.A.M. Dirac, Note on exchange phenomena in the Thomas atom, Math. Proc. Camb. Phil. Soc. 26 (1930) 376-385.

14 A.D. Becke, Density-functional thermochemistry. III. The role of exact exchange, J. Chem. Phys. 98 (1993) 5648-5652.

15 C. Lee, W. Yang, R.G. Parr, Development of the Colle-Salvetti correlation-energy formula into a functional of the electron density, Phys. Rev. B 37 (1988) 785-789.

16 J.-D. Chai, M. Head-Gordon, Long-range corrected hybrid density functionals with damped atom–atom dispersion corrections, Phys. Chem. Chem. Phys. 10 (2008) 6615-6620.

17 C.C.J. Roothaan, New developments in molecular orbital theory, Rev. Mod. Phys. 23 (1951) 69-89.

18 J.A. Pople, R.K. Nesbet, Self-consistent orbitals for radicals, J. Chem. Phys. 22 (1954) 571-72.

19 R. McWeeny, G. Dierksen, Self-consistent perturbation theory. 2. Extension to open shells, J. Chem. Phys. 49 (1968) 4852-4857.

20 J.A. Pople, R. Seeger, R. Krishnan, Variational configuration interaction methods and comparison with perturbation theory, Int. J. Quantum Chem., Suppl. Y-11 (1977) 149-163.

21 K. Raghavachari, H.B. Schlegel, J.A. Pople, Derivative studies in configuration-interaction theory, J. Chem. Phys. 72 (1980) 4654-4655.

22 K. Raghavachari, J.A. Pople, Calculation of one-electron properties using limited configuration-interaction techniques, Int. J. Quantum Chem. 20 (1981) 1067-1071.

23 Y. Zhao, D.G. Truhlar, The M06 suite of density functionals for main group thermochemistry, thermochemical kinetics, noncovalent interactions, excited states, and transition elements: two new functionals and systematic testing of four M06-class functionals and 12 other functionals, Theor. Chem. Account 120 (2008) 215-241.

24 S. Grimme, Semiempirical hybrid density functional with perturbative second-order correlation, J. Chem. Phys. 124 (2006) 034108-034116.

25 S. Grimme, S. Ehrlich, L. Goerigk, Effect of the damping function in dispersion corrected density functional theory, J. Comp. Chem. 32 (2011) 1456-1465.

26 L. Goerigk, S. Grimme, Efficient and accurate double-hybrid-meta-GGA density functionals—Evaluation with the extended GMTKN30 database for general main group thermochemistry, kinetics, and noncovalent Interactions," J. Chem. Theory Comput. 7 (2011) 291-309.

27 J. Tomasi, B. Mennucci, R. Cammi, Quantum mechanical continuum solvation models, Chem. Rev. 105 (2005) 2999-3093.

28 C. Møller, M.S. Plesset, Note on an approximation treatment for many-electron systems, Phys. Rev. 46 (1934) 0618-0622.

29 M. Head-Gordon, J.A. Pople, M.J. Frisch, MP2 energy evaluation by direct methods, Chem. Phys. Lett. 153 (1988) 503-506.

30 A.E. Reed, R.B. Weinstock, F. Weinhold, Natural-population analysis, J. Chem. Phys. 83 (1985) 735-746.

31 K.B. Wiberg, C.M. Hadad, T.J. LePage, C.M. Breneman, M.J. Frisch, An analysis of the effect of electron correlation on charge density distributions, J. Phys. Chem. 96 (1992) 671-679.

32 E.A. Gastilovich, V.G. Klimenko, N.V. Korol'kova, R.N. Nurmukhametov, Optical spectra and photophysical properties of polychlorinated dibenzo-*p*-dioxin derivatives, Russ. Chem. Rev. 69 (2000) 1037-1056.

33 E.A. Gastilovich, V.G. Klimenko, N.V. Korol'kova, G. Rauhut, Excited electronic states and effect of vibronic-spin–orbit coupling on the radiative deactivation of the lowest triplet states of dioxins, Chem. Phys. 270 (2001) 41-54.

34 I. Ljubić, A. Sabljić, Theoretical study of structure, vibrational frequencies, and electronic spectra of polychlorinated dibenzo-*p*-dioxins, J. Phys. Chem. A 110 (2006) 4524-4534.

35 E.A. Gastilovich, V.G. Klimenko, N.V. Korol'kova, R.N. Nurmukhametov, A nonradiative intersystem crossing $S(\pi\pi^*) \rightsquigarrow T(\pi\pi^*)$ transition in dibenzo-*p*-dioxin, Opt. Spectrosc. 105 (2008) 820-828.

36 E.A. Gastilovich, V.G. Klimenko, L.V. Volkova, R.N. Nurmukhametov, Nonradiative deactivation of the lowest excited triplet state of the dibenzo-*p*-dioxin molecule, Opt. Spectrosc. 111 (2011) 766-775.

37 E.A. Gastilovich, V.G. Klimenko, L.V. Volkova, R.N. Nurmukhametov, The role played by some factors of intramolecular interaction in nonradiative deactivation of the lowest triplet state of octachlorodibenzo-*p*-dioxin, Opt. Spectrosc. 113 (2012) 463-473.

38 E.A. Gastilovich, V.G. Klimenko, L.V. Volkova, R.N. Nurmukhametov, Nonradiative deactivation of the lowest triplet state of tetrachlorodibenzo-*p*-dioxin, Opt. Spectrosc. 116 (2014) 368-376.